Developmental Cell
Article

# Notch Signaling and Morphogenesis of Single-Cell Tubes in the *C. elegans* Digestive Tract

Jeffrey P. Rasmussen,[1,2,3] Kathryn English,[1,2] Jennifer R. Tenlen,[1,2,3] and James R. Priess[1,2,4,*]
[1]Fred Hutchinson Cancer Research Center, Seattle, WA 98109, USA
[2]Howard Hughes Medical Institute
[3]Molecular and Cellular Biology Program
[4]Department of Biology
University of Washington, Seattle, WA 98195, USA
*Correspondence: jpriess@fhcrc.org
DOI 10.1016/j.devcel.2008.01.019

## SUMMARY

**During organogenesis of the *C. elegans* digestive system, epithelial cells within a cyst-like primordium develop diverse shapes through largely unknown mechanisms. We here analyze two adjacent, dorsal epithelial cells, called pm8 and vpi1, that remodel their shapes and apical junctions to become donut-shaped, or toroidal, single-cell tubes. pm8 and vpi1 delaminate from the dorsal cyst epithelium and migrate ventrally, across the midline of the cyst, on a transient tract of laminin. pm8 appears to encircle the midline by wrapping around finger-like projections from neighboring cells. Finally, pm8 and vpi1 self-fuse to become toroids by expressing AFF-1 and EFF-1, two fusogens that are each sufficient to promote crossfusion between other cell types. Notch signaling in pm8 induces AFF-1 expression, while simultaneously repressing EFF-1 expression; vpi1 expresses EFF-1 independent of Notch. Thus, the adjacent pm8 and vpi1 cells express different fusogens, allowing them to self-fuse into separate, single-cell tubes while avoiding crossfusion.**

## INTRODUCTION

Epithelia formation is fundamental to the development of all animals. Epithelial cells are polarized, with basolateral domains separated from apical domains by adherens junctions. The adherens junctions contain E-cadherin and other proteins that mediate cell adhesion, and the basal surface typically is associated with a basal lamina. Despite the organization and cohesion of epithelial cells, epithelia can be extensively remodeled in response to developmental signals. Planar epithelia can be remodeled into tubes, and epithelial tubes can develop branches (Lubarsky and Krasnow, 2003). Although oriented cell division or apoptosis can contribute to remodeling (Gong et al., 2004; Schreiber et al., 2005), in many cases remodeling involves nondividing cells that change shape or position. For example, the elaborately branched tracheal tubes of *Drosophila* begin as sacs of epithelial cells that intercalate and change shape without dividing (Casanova, 2007). Epithelia can dissociate during epithelial to mesenchymal transitions (Thiery and Sleeman, 2006), or undergo transient restructuring to allow the passage of migrating cells. Examples of transepithelial migration include *Drosophila* germ cells that migrate through the posterior midgut epithelium to form the gonad (Kunwar et al., 2006), and the passage of human leukocytes through the epithelial lining of blood vessels to reach sites of infection (Petri and Bixel, 2006). These events demonstrate the remarkable ability of epithelial cells to change shapes by altering their adhesiveness.

The *C. elegans* pharynx provides an attractive model system for analyzing molecular mechanisms of epithelial remodeling during organogenesis. The pharynx is essentially a monolayered myoepithelial tube whose anatomy, specification, and gene expression have been compared to the heart of higher animals. For example, the ascidian heart is a simple tube, consisting of a monolayer of myoepithelial cells (Oliphant and Cloney, 1972). The NK homeodomain transcription factors CEH-22 and Nkx2.5 function in nematode pharynx and vertebrate heart development, respectively, and zebrafish Nkx2.5 can rescue *C. elegans* mutants lacking CEH-22 (Chen and Fishman, 1996; Okkema and Fire, 1994; Okkema et al., 1997; Haun et al., 1998). In addition to muscle cells, the pharynx contains glands, neurons, and structural cells called marginal cells. An ultrastructural reconstruction of the adult pharynx showed these individual cells have remarkably complex and reproducible shapes (Albertson and Thomson, 1976). Along the longitudinal axis of the pharynx, muscles and marginal cells are organized into distinct anterior/posterior groups based on region-specific morphologies. For example, the most anterior muscle is shaped like a fenestrated cylinder with openings that are nearly as large as the cell, while the most posterior muscle is a toroid. The pharynx is linked to the intestine through valve cells, the first of which is also a toroid.

Nearly all of the complex changes in pharyngeal cell shape begin within a cylindrical cyst of initially uniform, simple epithelial cells (Leung et al., 1999; Portereiko and Mango, 2001). During early embryogenesis, cells from two separate lineages aggregate to form a primordium that forms the pharynx and valve (reviewed in Mango, 2007). In both lineages, the key step in specifying pharyngeal/valve fate is the expression of *pha-4*, an organ selector gene that encodes a forkhead box transcription factor. PHA-4 is expressed in all pharyngeal and valve cells, and is necessary and sufficient for most early embryonic cells to adopt pharyngeal fates (Horner et al., 1998; Kalb et al.,

1998; Mango et al., 1994). Midway through embryogenesis, cells in the primordium polarize to form an epithelial cyst that is primarily one cell in thickness (Leung et al., 1999). In cross-sections of the cyst, most cells have a simple, wedge-shaped appearance: each cell has a narrow apical tip facing the midline of the cyst, and a broad basal surface associated with a basal lamina.

A complex remodeling of the cyst occurs over the next few hours of embryogenesis (Leung et al., 1999; Mango, 2007). The cylindrical cyst is transformed into a bilobed tubular pharynx that contains a wide diversity of cell shapes and that is partitioned from the adjacent valve cells by a basal lamina. To understand how cell shapes are determined within the cyst, we analyzed here the development of two toroidal, single-cell tubes called pm8 and vpi1. We show that morphogenesis involves Notch signaling, epithelial to mesenchymal transitions, migration through neighboring cells on a transient tract of laminin, and self-fusion. These results reveal numerous interactions that contribute to the final shapes of the cells.

## RESULTS

### Background

The pharynx is a bilobed myoepithelial tube containing pharyngeal muscles (pm), structural cells called marginal cells (mc), gland cells, and neurons (Figure 1A; see Mango, 2007 for description of pharyngeal anatomy and development). The pharynx connects to the intestine through a multicellular valve (vpi cells for *v*alve *p*harynx/*i*ntestine). The events analyzed here occur in the posterior lobe of the pharynx, called the terminal bulb, and in the adjacent valve cells. Most cells in the pharynx are arranged with 3-fold radial symmetry around the lumenal axis (Figure 1A and Movie S1, see the Supplemental Data available with this article online). Muscles, marginal cells, and valve cells show anterior/posterior differences in cell morphology, creating distinctive groups of one to six cells (groups pm1–8, mc1–3, vpi1–3; Albertson and Thomson, 1976). For example, mc3V is the ventral cell of the three group 3 marginal cells (Figure 1A). Although multiple cells surround the lumen of the pharynx/valve in a typical cross-section, there are two examples of single-cell tubes: pm8, the terminal cell in the pharynx, and vpi1, the first cell in the valve (Figures 1A–1C). Our analysis of pm8 and vpi1 morphogenesis begins at about 6.5 hr after the two-cell stage of embryogenesis, when the primordium of the pharynx/valve is a cylindrical cyst of polarized epithelial cells (Figures 1B and 1D). The apical surfaces of these cells face the midline of the cyst, where the pharyngeal/valve lumen forms, and are outlined by junctional proteins such as AJM-1 (Figures 1D and 1E). The basal surfaces of these cells face the periphery of the cyst and are associated with a basal lamina that contains laminin (Figure 1D).

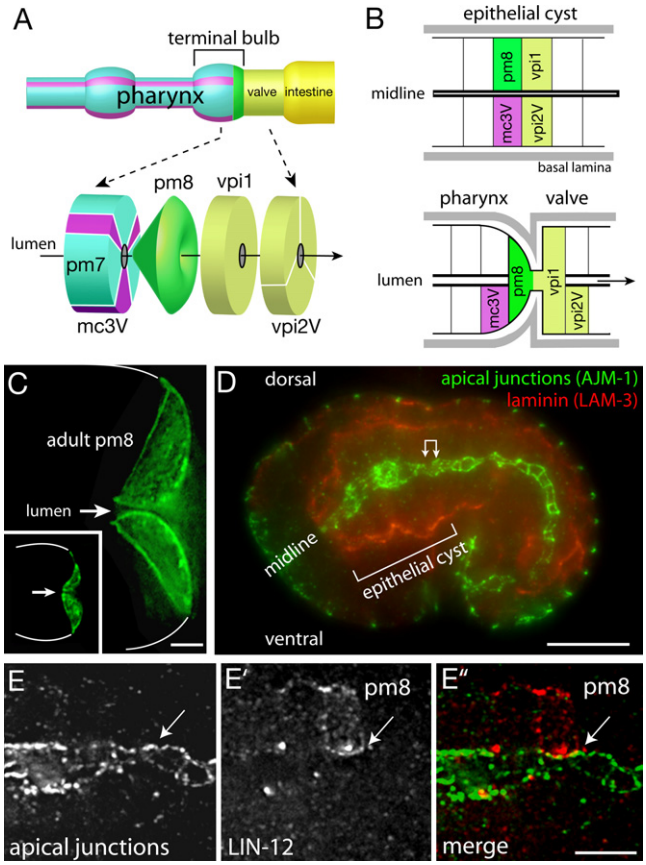


**Figure 1. Cell Morphology and Polarity in the Pharynx/Valve**

(A) Diagram of some of the cells in the terminal bulb of the pharynx and in the valve. The three group 3 marginal cells are shown in purple, and names of the principle cells mentioned in the text are indicated.

(B) Diagram of cell positions in the cyst (top) and pharynx/valve (bottom). Note the reorientation of the basal lamina-associated, basal surfaces of pm8 and vpi1.

(C) pm8 in an adult and newly hatched larva (inset) visualized by *ref-1*::GFP-PM; white lines indicate perimeter of terminal bulb.

(D) Optical longitudinal section through the middle of an embryo showing the epithelial cyst (bracket).

(E–E″) High magnification of region corresponding to double-headed arrow in (D) after immunostaining for apical junctions (AJM-1) and LIN-12/Notch to visualize pm8 (see also Figure 3D). Note that pm8 contacts, but does not cross, the midline (arrow). Polygonal shapes are the apical surfaces of various cells in the cylindrical array around the midline. Bars = 2 μm (C), 10 μm (D), and 2.5 μm (E–E″).

### Notch Signaling Regulates Gene Expression in pm8

Several genes have been described that are expressed in multiple or all pharyngeal and valve cells, however, the *ceh-24* gene is expressed uniquely in pm8 (Harfe and Fire, 1998). CEH-24 is an NK transcription factor related to CEH-22 (see Introduction), and previous studies identified a 117 bp enhancer from *ceh-24* that promotes pm8-specific expression (Harfe and Fire, 1998). We noticed that this enhancer contained a conserved GTGGGAA sequence that is a predicted binding site for LAG-1/CSL, the core DNA-binding protein in the Notch signaling pathway (Figure S1A; see Greenwald, 2005 and Bray, 2006 for reviews on Notch). We found that LAG-1/CSL bound the wild-type enhancer in vitro, and that binding was dependent on the GTGGGAA sequence (Figure S1B). Transgenic *ceh-24*::GFP reporters constructed with either the wild-type enhancer sequence, or with a GTGGGAA to GAGGCAA mutation, were expressed in head neurons outside the pharynx, but only the wild-type enhancer drove robust expression in pm8 (Figure 2C and Figure S1D; Table 1). Expression was dependent on Notch activity, as *lin-12 glp-1* double mutants that lack both of the *C. elegans* Notch proteins, LIN-12 and GLP-1, either did not express *ceh-24*::GFP (18/20 embryos)

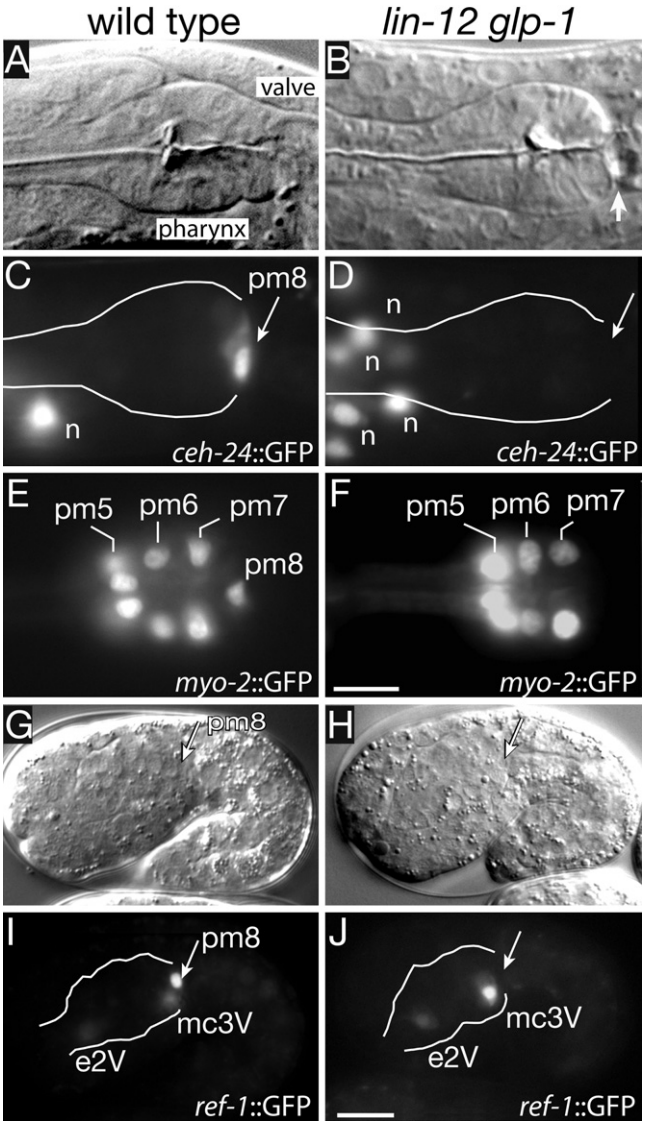


**Figure 2. Notch-Dependent Gene Expression in pm8**

The columns show wild-type (left) and *lin-12 glp-1* mutant (right) animals either after hatching at 14 hr (A–F), or at 7 hr in embryogenesis (G–J). Transgenic reporters are as listed; white lines indicate perimeter of the pharynx (C and D) or epithelial cyst (I and J). Nuclei labeled "n" in (C) and (D) are neurons outside the pharynx that express *ceh-24*::GFP. Bars = 5 μm (A–F), and 10 μm (G–J). Embryos are approximately 50 μm in length.

or showed only weak expression (2/20 embryos; Figure 2D; Table 1).

REF-1 is a *C. elegans* bHLH transcription factor that is distantly related to *Drosophila* E(spl) (Alper and Kenyon, 2001; Neves and Priess, 2005). The *ref-1* gene is a direct target of Notch signaling in several interactions in the early embryo, but is expressed in other cells independent of Notch (Neves and Priess, 2005). In the wild-type epithelial cyst, we found that *ref-1*::GFP was expressed in pm8 and in the sister cells e2V and mc3V (Figure 2I and data not shown). *lin-12 glp-1* double mutants showed expression in e2V and mc3V, but not in pm8 (Figure 2J; Table 1). Additional experiments showed that pm8 expression required LAG-1/CSL, and appeared to involve either of the Notch ligands LAG-2/Delta or APX-1/Delta (Table 1 and see below).

The *myo-2* gene encodes a pharyngeal-specific myosin; the *myo-2* promoter lacks predicted LAG-1/CSL binding sites, and thus is unlikely to be a direct target of Notch signaling (data

**Table 1. Transgene Expression in pm8**

| Reporter | Genotype | pm8 Expression % (n)[a] |
|---|---|---|
| ceh-24*::GFP* | *WT* | 100 (50) |
| | *lin-12(n676n930ts)* | 52 (72) |
| | *lin-12(n941)glp-1(q46)* | 10 (20) |
| ceh-24$^{(-CSL)}$*::GFP* | WT | 15 (38)[b] |
| *ref-1*$^{(1.8kb)}$::REF-1::GFP | *WT* | 100 (60) |
| | lin-12(n941)glp-1(q46) | 0 (83) |
| | lin-12(n941) | 2 (64) |
| *ref-1*$^{(600bp)}$::GFP | *WT* | 100 (35) |
| | lag-1(q385)/+ | 100 (18) |
| | *lag-1(q385)* | 0 (10) |
| | *lag-2(q411)* | 100 (15) |
| | *lag-2(q420ts)* | 100 (20) |
| | *apx-1(zu347ts)* | 100 (21) |
| | lag-2(q387)[c] | 0 (12) |
| *ref-1*$^{(1.8\ -CSL)}$::REF-1::GFP[d] | *WT* | 0 (25) |
| *myo-2*::GFP | WT | 100 (110) |
| | *lag-2(q420ts)* | 100 (36) |
| | *lin-12(n941)/+* | 100 (44) |
| | *lin-12(n941)* | 36 (78) |
| | *lin-12(n941)glp-1(q46)*[e] | 45 (206)[f] |
| | *lag-1(q385)* | 3 (89) |
| *aff-1*::GFP[g] | WT | 96 (67) |
| | *lag-1(q385)* | 2 (62)[h] |

[a] Expressing cells at or near the normal position of pm8 were scored as positive; this includes cases where the expressing cell was in the valve. For example, 9/93 *myo-2*::GFP-expressing nuclei in *lin-12(n941)glp-1(q46)* were in the valve adjacent to the pharynx.
[b] Expression was weak and in two cases a comparable signal was observed in vpi1.
[c] *lag-2(q387)* is a small deficiency that deletes both *lag-1* and *apx-1*, but removes several additional genes.
[d] This reporter lacks all eight CSL sites (Neves and Priess, 2005).
[e] These animals showed a strong correlation between *myo-2*::GFP expression and whether or not the pm8 nucleus was in the ventral side of the terminal bulb; 38/57 of expressing pm8 cells were ventral.
[f] The myogenesis defect in *lin-12 glp-1* double mutants is significantly less than in *lag-1* mutants. Additional experiments ruled out the possibility that the candidate pm8 muscle was a different cell that normally undergoes apoptosis (see analysis in Figure S2). Because the homozygous *lin-12 glp-1* larvae were derived from heterozygous parents, perdurance of maternally-provided *lin-12* and/or *glp-1* might contribute to the phenotype. However, the phenotype of the double mutant was not enhanced by *lin-12(RNAi)*, and it is not possible to remove maternal *glp-1* without severely disrupting embryogenesis (data not shown; Priess, 2005).
[g] Because this reporter transgene is not integrated into a chromosome, and can be lost spontaneously, only those animals with expression in the pm3 and pm5 muscle groups of the pharynx were scored for pm8 expression.
[h] The single positive animal had expression throughout the valve.

not shown). We generated an integrated transgenic strain expressing a nuclear-localized *myo-2*::GFP reporter (J. Gaudet, unpublished data), and found that wild-type larvae reproducibly showed expression in each of the expected 13 muscle nuclei in the terminal bulb (6 pm5 + 3 pm6 + 3 pm7 + 1 pm8; Figure 2E; Table 1). Notch mutant larvae had defects in pm8 myogenesis (Figure 2F and Figure S2B); for example, 97% of *lag-1* mutant larvae contained only 12 *myo-2*::GFP-expressing cells in the terminal bulb, and specifically lacked expression at the normal position of pm8 (Table 1). We conclude that Notch signaling induces the expression of a least two transcription factors in pm8, CEH-24 and REF-1, and is required for pm8 myogenesis.

## Notch Mutants Are Defective in Both pm8 and vpi1 Morphogenesis

*lag-1* mutant larvae usually lacked a nucleus in the normal position of the pm8 nucleus, suggesting that Notch mutants have a defect in pm8 morphogenesis that is at least partially separate from the myogenesis defect. We used light and electron microscopy to compare the pharynx and valve in newly hatched, wild-type larvae with Notch mutant larvae. In newly hatched, wild-type larvae, the first valve cell (vpi1) forms a cup-like enclosure over the posterior end of pm8 (Figures S3A and S3C); in live animals, pm8 and vpi1 appear tightly adherent and show no visible separation during body locomotion (unpublished data). pm8 and vpi1 make a small direct contact near their apical surfaces, but are otherwise separated by a prominent basal lamina that almost completely separates the pharynx from the valve (Figure S3C). In Notch mutant larvae, cells at the pharynx/valve interface had several morphological defects including large gaps between cells (arrow in Figure 2B), broad contacts between pharyngeal cells and valve cells without an intervening basal lamina (Figure S3B and data not shown), and abnormal patterns of apical junctions (see Figures 4H and 4I). We were unable to identify cells with the normal morphology of pm8 or vpi1 in the mutant larvae, although other cells such as the pm6 and pm7 muscles appeared well differentiated (n = 12; Figure S3B). Thus, these results suggest the Notch pathway has a role in the differentiation or morphogenesis of pm8, vpi1, and possibly other valve cells.

## Notch Is Activated in the Postmitotic pm8 Cell

To determine when and where Notch interactions occurred, we first sought to identify the relevant ligand-expressing cells through laser-killing experiments. We found that descendants of the embryonic cell MSaapa that were not previously known to function in Notch signaling expressed the ligand LAG-2/Delta (Figure 3A) and were required for Notch-dependent *ref-1*::GFP expression in pm8 (Figure 3B). In immunostaining experiments, the first apparent contact between MSaapa descendants expressing *lag-2*::GFP and cells that express the receptor LIN-12/Notch occurred after the birth of pm8, approximately 6 hr after the two-cell stage. A clone of four LIN-12-expressing cells is located in the left dorsal quadrant of the epithelial cyst; the most posterior cell in this group is pm8 (Figures 3C and 3D). At this stage, vpi1 is in the right dorsal quadrant of the cyst and does not express detectable levels of LIN-12; the receptor GLP-1/Notch was not detectable in vpi1 or pm8 (Figure 3C and data not shown). MSaapa descendants within the cyst express LAG-2/Delta, and one or two of these cells contact pm8 directly (Figure 3C). Lateral views of embryos at approximately the same stage showed Notch-independent expression of *ref-1*::GFP in the pharyngeal cells e2V and mc3V, but no other pharyngeal or valve cells (Figure 3D′). However, pm8 showed strong *ref-1*::GFP expression about 30 min later (Figure 3E′). These results suggest that Notch signaling is activated in the postmitotic pm8 cell, but not in vpi1 or any other valve cell, and that Notch thus has an indirect role in valve differentiation or morphogenesis.

## pm8 and vpi1 Morphogenesis

The initial stages of wild-type pm8 morphogenesis were visualized by immunostaining for LIN-12/Notch. For subsequent stages, we used the *ref-1* promoter to drive expression of a plasma membrane-localized GFP (*ref-1*::GFP-PM). pm8 initially is a wedge-shaped epithelial cell on the dorsal, left side of the cyst, and has a broad, midline-facing apical surface similar to other cyst cells (Figures 1E and 3D). Shortly thereafter, pm8 nearly detaches from the dorsal basal lamina, and its apical surface is remodeled into a lamella that invades the ventral side of the cyst (Figures 3E, 4A, and 4B; data not shown). Both the pm8 nucleus and bulk cytoplasm cross into the ventral side, leaving only a thin connection to the dorsal perimeter of the cyst (Figures 4A–4D). pm8 invades the ventral side of the cyst to the left of the midline, but gradually spreads across the entire cross section of the cyst (Figure 4F and Movie S1).

vpi1 morphogenesis was examined by electron microscopy and expression of *eff-1*::EFF-1::GFP (see below). Similar to pm8, vpi1 initially is a wedge-shaped dorsal cell that extends a lamellar process into the ventral side of the cyst; the vpi1 lamella is closely associated with the posterior surface of the migrating pm8 cell body (Figure 4E and Figure S3D). In contrast to pm8, the nucleus and bulk cytoplasm of vpi1 remain on the dorsal side of the cyst. Both pm8 and vpi1 appear to redistribute cytoplasm throughout their respective cell bodies during late embryogenesis, becoming symmetrical tubes centered on the midline of the cyst (Figure 1C, inset, and data not shown).

## pm8 and vpi1 Migrate within the Cyst on a Transient Path of Laminin

In all embryos analyzed, pm8 and vpi1 migrated into the ventral side of the cyst specifically at the lateral interface between the ventral cells mc3V and vpi2V (see Figure 1B). In some examples of transepithelial migration in other systems, cells in the target epithelium disassociate prior to the arrival of migrating cells, thus creating openings for migration (Kunwar et al., 2006). Electron micrographs of the epithelial cyst before or during pm8 migration did not show obvious gaps between any ventral cells (data not shown). A second possibility is that the mc3V/vpi2V interface provides a guidance cue for pm8 migration. Consistent with this hypothesis, we found that a transient tract of laminin appears in the ventral cyst shortly before pm8 migration (Figures 5A and 5D), and disappears after pm8 migration (Figure 5E). Heterotrimeric laminin in *C. elegans* is composed of either of two $\alpha$ chains (EPI-1 and LAM-3), a $\beta$ chain (LAM-1), and a $\gamma$ chain (LAM-2) (Kramer, 2005). An antiserum specific for LAM-3 stained the tract in wild-type embryos, but not in *lam-3* mutant embryos (data not shown). In time-lapse movies of *lam-1*::LAM-1::GFP, the laminin tract appeared to spread inward from the ventral perimeter of the cyst over a 20 min interval (Movie S2) before regressing. In later

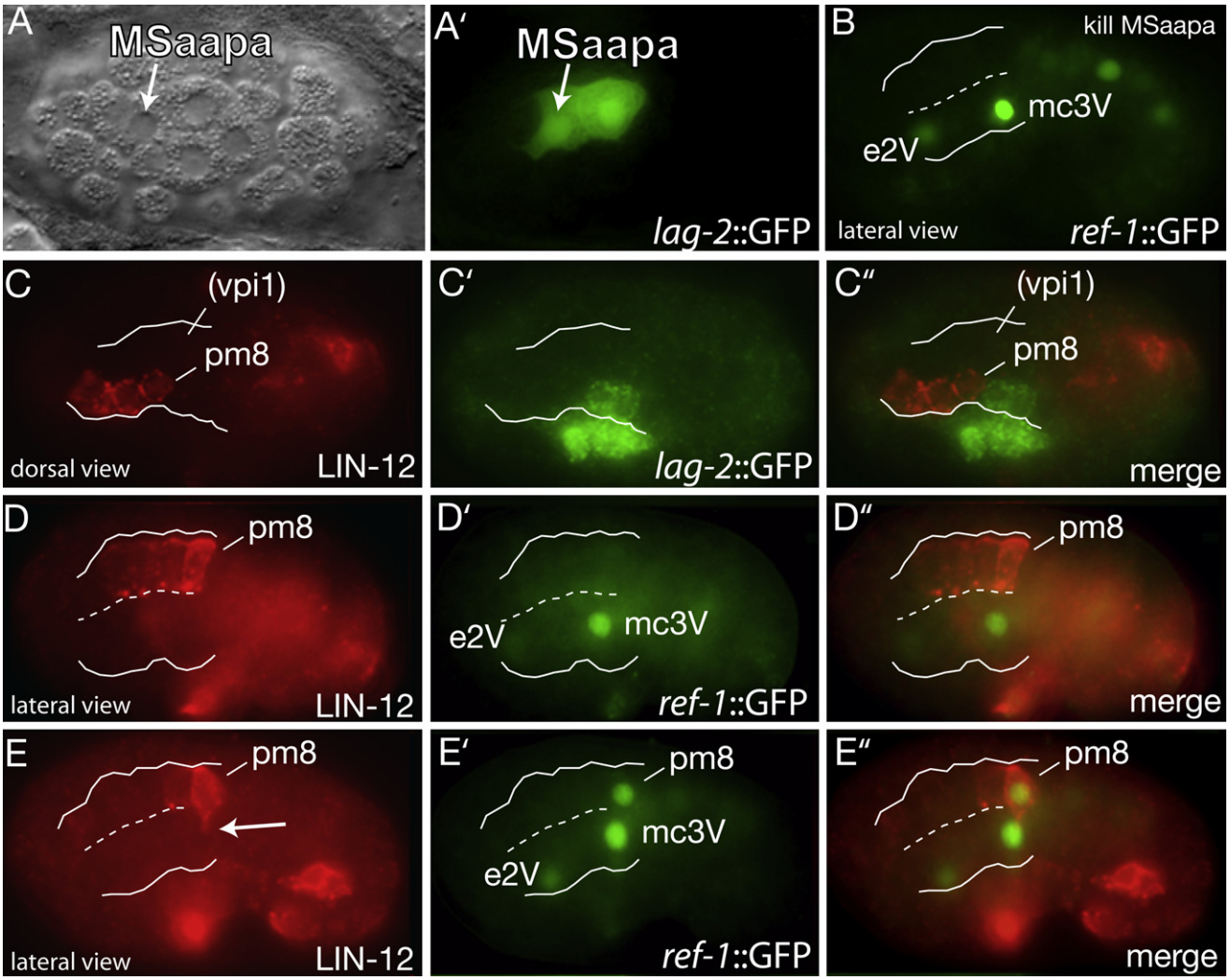


**Figure 3. Notch Signaling in the Epithelial Cyst**

(A–A′) Ventral view of an embryo before formation of the cyst showing *lag-2* expression in MSaapa.

(B) *ref-1*::GFP expression in a cyst-stage, wild-type embryo after killing MSaapa; embryo shown is the same stage and orientation as in Figure 2I. *ref-1*::GFP expression in pm8 was observed after killing the following cells: MS (0/4 embryos), MSaa (0/4- MS and MSaa are precursors of pm8), MSap (6/6), MSaap (0/4), MSaapa plus MSaapp (0/3), MSaapp (5/5),and MSaapa (4/4 when the ablated cell entered the body cavity, 0/3 when it remained outside).

(C–C″) Dorsal view of a 6 hr embryo immunostained for GFP (*lag-2*::GFP) and LIN-12/Notch; white lines indicate boundary of epithelial cyst. The approximate position of vpi1 is indicated based on light microscopy of living embryos at this stage and orientation.

(D–D″) Lateral view of embryo at about the same stage as (C); *ref-1*::GFP is expressed in the Notch-independent cells e2V and mc3V, but not in pm8.

(E–E″) Embryo approximately 20 min later than in (D) showing *ref-1*::GFP in pm8. Note lamella from pm8 (arrow in [E]) extending ventrally across the midline of the cyst (dashed line).

embryogenesis, a different and permanent zone of laminin appears along the posterior surface of pm8 that is part of the basal lamina between pm8 and vpi1 (Figure 5F and Figure S3C). Using *ref-1*::GFP to identify both mc3V and pm8, we found that the transient laminin tract appeared specifically at the mc3V/vpi2V interface, and that the tract disappeared concomitant with the ventral migration of pm8 (Figures 5G–5I). The laminin tract was present at the mc3V/vpi2V interface in *lin-12 glp-1* mutants, indicating that it is specified independent of Notch signaling. Indeed, the tract persisted in 7.5 hr-old *lin-12 glp-1* mutant embryos (Figure 5B) long after it disappears from wild-type embryos (Figure 5E).

An antiserum against EPI-1 stained the tract, indicating that it contains both laminin $\alpha$ chains, LAM-3 and EPI-1. We found that *lam-3* and *epi-1* single mutants appeared to have normal pm8 migration (data not shown). However, pm8 was unable to migrate ventrally in *lam-3; epi-1* double mutants, and instead remained primarily on the dorsal side of the cyst (Figure 5J). Cell migration on laminin surfaces can involve the major laminin receptor, integrin. In *C. elegans*, *ina-1* is one of two genes encoding the $\alpha$ subunit of heterodimeric integrin, and *pat-3* encodes the sole $\beta$ subunit (Kramer, 2005). *pat-3(RNAi)* embryos had severe developmental defects that complicated an analysis of pm8 migration. However, most *ina-1* mutants were able to

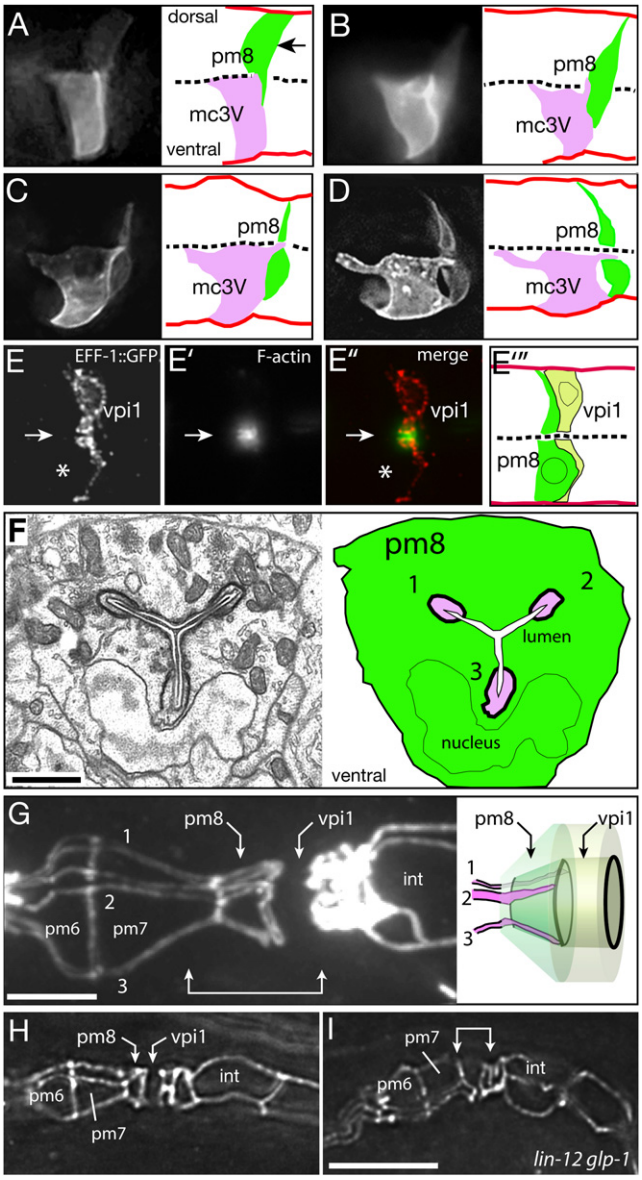


**Figure 4. Ventral Migration and Lumen Formation in pm8 and vpi1**

(A–D) *ref-1*::GFP-PM expression in pm8 and the group 3 marginal cell mc3V in successively older embryos. Images are optical sections through the midline of the cyst; a complete image series corresponding to (D) is shown in Movie S4.

(E–E″) vpi1 expressing *eff-1*::EFF-1::GFP and stained with phalloidin to visualize F-actin at the midline (arrow); note relative absence of actin in pm8 (asterisk indicates position of pm8 nucleus).

(E‴) Diagram of vpi1 with the approximate position of the pm8 cell body included for reference (see Figure S3D).

(F) Electron micrograph and diagram of a cross-section through pm8 in an embryo near hatching. The three marginal cell fingers (numbered 1–3) are evident in the Y-shaped lumenal channel (white) of pm8.

(G) Apical junctions in a wild-type, third stage (L3) larva; cells in the pharynx and valve do not divide during larval development, but increase in size and allow better visualization of apical junctions. Apical surfaces of cell like pm7 resemble broad triangles, while the group 3 marginal cells (numbered 1–3) have long, thin apical surfaces (see also Movie S1). Note how fingers from the marginal cells extend through the apical surface of pm8. The region indicated by the double-headed arrow is diagrammed to show a superposition of the pm8 and vpi1 cell bodies on their apical surfaces; apical junctions are drawn in black. (H and I) Same region as in (F) in wild-type (H) and *lin-12 glp-1* mutant (I) embryos near hatching. Bars = 1 μm (F) and 5 μm (G–H).

complete embryogenesis and hatch as deformed larvae. We found that *ina-1* mutants showed severe defects in pm8 migration (Figure 5K). In many larvae, pm8 appeared to have migrated abnormally into the region normally occupied by valve cells and anterior intestinal cells (Figure 5K). The pm8 cell body was closely apposed to the basal lamina surrounding the valve and intestine, suggesting that pm8 might extend along basal laminae associated with these surfaces rather than the normal mc3V/vpi2V interface.

## Tubulogenesis and Self-Fusion

A single-cell tube such as pm8 or vpi1 might, in principle, be either a toroid or a C-shaped cell. The apical surfaces of both types of tubes have circular intercellular junctions at each end of the cell, but only the C-shaped cell has an autocellular apical junction (Figure 6A). pm8 and vpi1 have been shown to be toroids, rather than C-shaped cells, in adult *C. elegans* (Albertson and Thomson, 1976). We found that in 7.5 hr embryos pm8 and vpi1 had the apical junction pattern expected for toroidal cells (two unconnected circles; Figure 6B), and confirmed by electron microscopy that both cells are toroids (Figure S4). Although an epithelial cell can roll up into a C-shape, a toroid has a distinct topology that requires at least one self-fusion event. *C. elegans* development provides multiple examples where adjacent cells fuse together into a multinucleate syncytium, and most of these fusions require the *eff-1* gene (Mohler et al., 2002). EFF-1 acts homotypically to induce fusion; it is sufficient to promote fusion of heterologous cells that each express EFF-1 (Podbilewicz et al., 2006). Recent studies in *C. elegans* have identified a second fusogen, AFF-1, with a similar ability to fuse heterologous cells (Sapir et al., 2007). We found that *eff-1*::EFF-1::GFP was expressed at high levels in vpi1 beginning at about 7 hr (Figure 6B′), but was never expressed in pm8. In 7.5 hr *eff-1* mutant embryos, vpi1 had a novel, autocellular junction as characteristic of a C-shaped cell, while pm8 retained the wild-type, toroidal pattern of intercellular junctions (Figure 6B, inset). Conversely, *aff-1*::GFP was expressed in the wild-type pm8 beginning at about 7.2 hr, but was never expressed in vpi1 (Figure 6C′). In 7.5 hr *aff-1* mutant embryos, pm8 had a novel autocellular junction, while vpi1 retained the wild-type, toroidal pattern of intercellular junctions (Figure 6B, inset). These results suggest that in normal development both pm8 and vpi1 adopt C-shapes before self-fusing through AFF-1 and EFF-1 activities, respectively.

Because cells in the approximate positions of pm8 and vpi1 have highly abnormal patterns of apical junctions in Notch mutants, we examined EFF-1 expression in these embryos. Although *eff-1*::EFF-1::GFP is expressed only in vpi1 in wild-type embryos, in *lag-1* mutant embryos the reporter was expressed in two adjacent cells at this position (Figures 6D and 6E), or in a single, abnormally large binucleate cell (Figure 6F). We identified one of the cells that expressed *eff-1*::EFF-1::GFP as pm8 based on its contact with group 7 muscle cells (data not shown). Conversely, neither pm8 nor vpi1 expressed *aff-1*::GFP in *lag-1* mutants (Table 1). We conclude that Notch has two roles in pm8 and vpi1 tubulogenesis. First, Notch is required for pm8 to express AFF-1, allowing pm8 to self-fuse. Second, Notch is

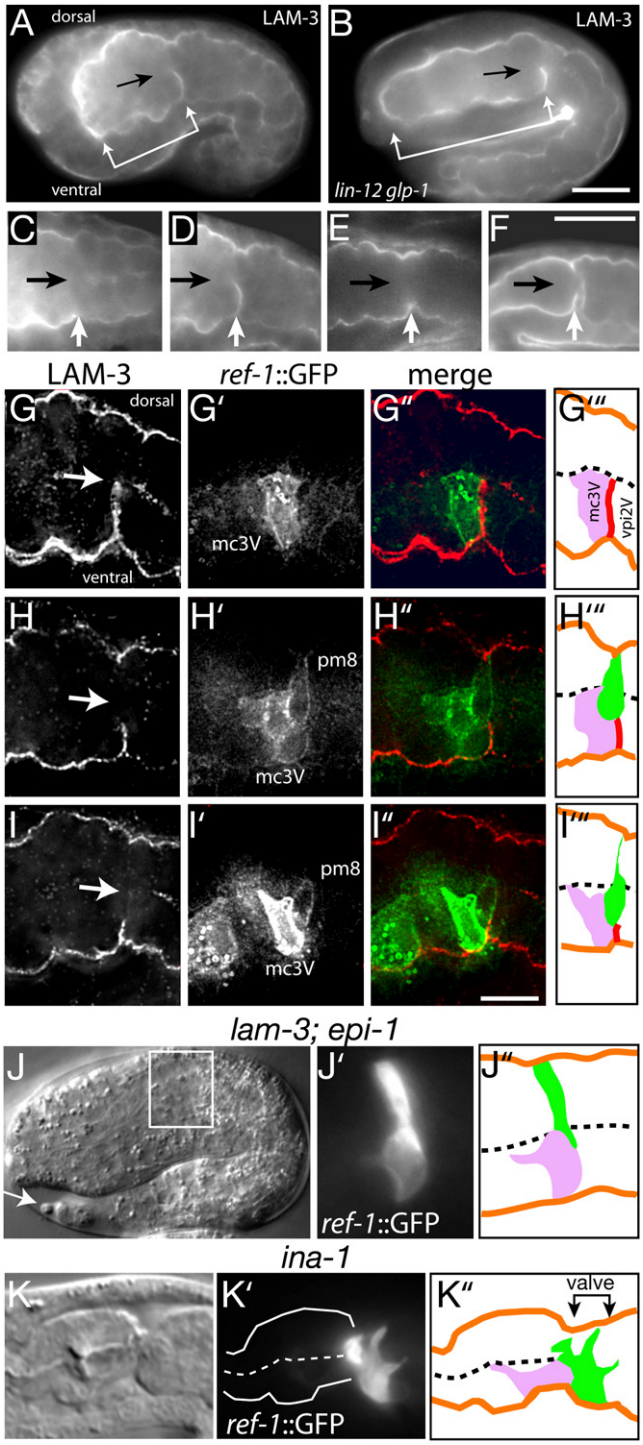


**Figure 5. pm8 Migrates Ventrally on a Laminin Tract**

(A) Optical longitudinal section through the middle of a 7 hr embryo stained for laminin. Laminin is present in the basal lamina surrounding the cyst (bracket). A transverse tract of laminin is evident in the posterior ventral half of the cyst (arrow indicates the cyst midline).

(B) *lin-12 glp-1* embryo at 7.5 hr.

(C–F) Sequence of successively older wild-type embryos showing the appearance (D) and disappearance (E) of the laminin tract, followed by the deposition of laminin on the posterior surface of pm8 after morphogenesis (F).

(G–I) Single embryos immunostained for LAM-3 and GFP (*ref-1*::GFP-PM) before (G), during (H), and near the completion (I) of pm8 migration. Arrows indicate the midline of the cyst. The fixation required for LAM-3 staining compromises GFP-PM localization in pm8 (compare with Figures 4A–4D).

(J) *lam-3; epi-1* double mutant at about 9 hr; pm8 has failed to migrate to the ventral side. This embryo has a shape similar to younger, 7.5 hr wild-type embryos because of defects in body morphogenesis, but has the well-formed tail spike (arrow) characteristic of wild-type 9 hr embryos.

(K) *ina-1* mutant larva showing pm8 extension into the valve/anterior intestine; similar defects occur in 74% of the hatched animals (n = 46). Bars = 10 μm (A–F) and 5 μm (G–I).

required to prevent pm8 from expressing EFF-1, thereby preventing pm8 from crossfusing with the EFF-1-expressing vpi1 cell.

### Formation of the Intracellular Lumen in pm8 and vpi1

If pm8 and vpi1 normally become C-shaped cells that then self-fuse into toroids, how are their C-shapes determined? Three group 3 marginal cells are immediately anterior to pm8 during pm8 and vpi1 morphogenesis, and one of these (mc3V) expresses the same *ref-1*::GFP-PM reporter as pm8 (see Figures 1A and 3E′). In analyzing pm8 morphogenesis, we discovered that all three marginal cells extend a finger-like process posteriorly along the midline of the cyst during pm8 and vpi1 morphogenesis (Figures 4A–4D, and 4F, Figure S4A, and Movie S3). Thus, as the pm8 cell body moves into the left ventral side of the cyst, then spreads across the entire cross-section of the cyst, it wraps around the three marginal cell fingers (Movie S4). The fingers appeared to stop at, or extend slightly beyond, the posterior surface of pm8, where they would presumably contact the thin, ventral lamella from vpi1; vpi1 showed a strong enrichment of filamentous actin at the midline during formation of its lumen that was not apparent in pm8 (Figure 4E). Previous studies have shown that the pharyngeal lumen begins as small opening along the midline of the epithelial cyst; as the lumen expands it acquires a Y-shape when viewed in cross-section (Leung et al., 1999). The three marginal cell fingers remained in the center of pm8 during lumenal expansion, moving apart to occupy the three tips of the Y-shaped lumen (Figure 4F). The marginal cell fingers formed apical junction connections with the apical face of pm8, but not vpi1, and persisted in the pm8 cell body throughout larval development. Thus, while the cylindrical apical surface of pm8 initially has only two circular intercellular junctions (Figure 6B), in late embryos and larvae there are an additional three paired lines of junctional material across this surface that correspond to the three fingers (Figure 4G and 4H). An intriguing possibility is that the marginal cells fingers template the lumenal channel through pm8, and possibly vpi1, as pm8 and vpi1 remodel their apical surfaces. However, we have not yet been able to test this hypothesis by removing all three marginal cells simultaneously; pm8 formed an abnormally shaped lumen when only mc3V was killed with a laser microbeam (2/2 embryos), or when the fate of mc3V was transformed by the *glp-1(e2072)* mutation (3/3 embryos examined by electron microscopy; see Priess et al., 1987).

## DISCUSSION

### Establishment of the Pharynx/Valve Boundary

We here analyzed the morphogenesis of pm8 and vpi1, two adjacent, single-cell tubes in the *C. elegans* digestive tract. pm8

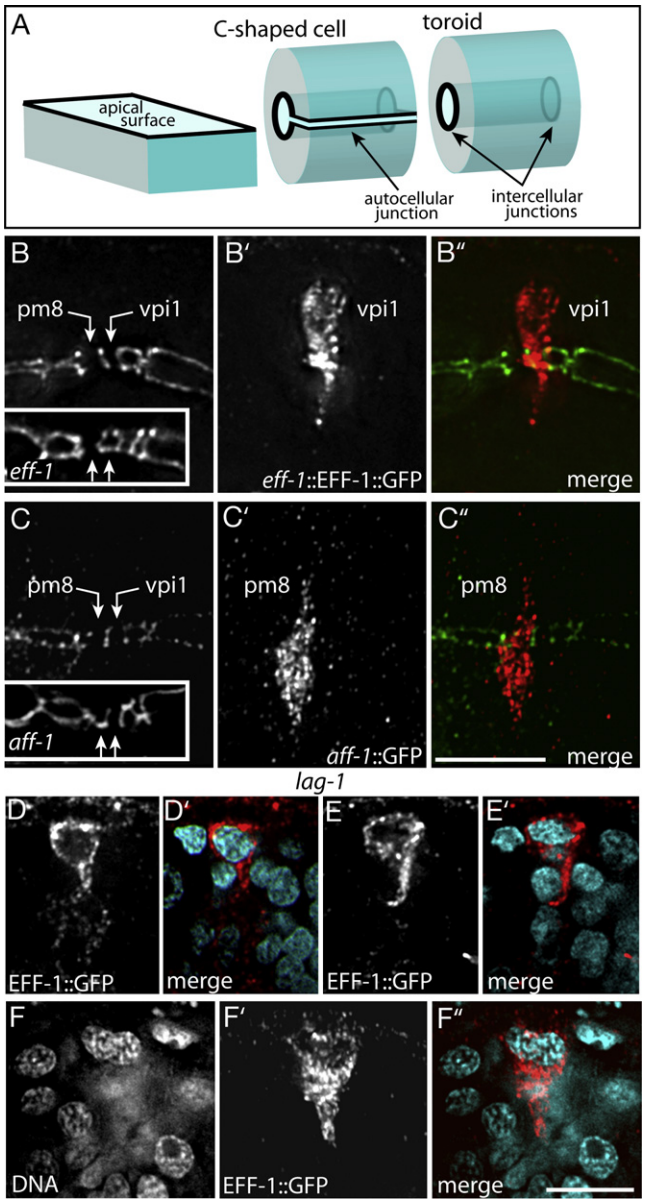


**Figure 6. Self-Fusion of pm8 and vpi1**

(A) Diagram comparing (1) a box-like cell with a simple, flat apical surface, (2) a topologically equivalent C-shaped cell, and (3) a topologically distinct toroid with a cylindrical apical surface; apical junctions are shown as bold lines.

(B–B″) Apical junctions at the pharynx/valve boundary in a 7.5 hr wild-type embryo stained for the apical junction marker AJM-1 (B) and for *eff-1*::EFF-1::GFP (B′). In this longitudinal view, the intercellular junctions at the ends of pm8 and vpi1 appear as vertical lines (B). The inset in (B) shows the same region in an *eff-1* mutant with an autocellular junction linking the intercellular junctions in vpi1, but not pm8.

(C–C″) Same region and stage as in (B), showing *aff-1*::GFP expression in pm8 and an autocellular junction in pm8 in an *aff-1* mutant (inset).

(D and D′) *lag-1* embryo showing a mononucleate cell expressing *eff-1*::EFF-1::GFP.

(E and E′) Different focal plane of the same embryo in (D) showing a second *eff-1*::EFF-1::GFP-expressing cell. Note that both cells have a ventral-directed process but neither cell extends completely through the cyst.

(F–F″) *lag-1* embryo with binucleate cell expressing *eff-1*::EFF-1::GFP.

Bars = 2.5 μm (B–F).

and vpi1 differentiate within a cyst of initially similar epithelial cells that all express PHA-4. The morphogenetic events that define the pm8/vpi1 boundary compartmentalize the cyst into the functionally distinct organs of the pharynx and valve. Cells throughout the epithelial cyst initially have radially oriented apicobasal axes, and most cells retain this polarity after morphogenesis. For example, pharyngeal muscles have single sarcomeres, and in most of these muscles the myofilaments are oriented radially, extending from the pharyngeal lumen to the peripheral basal lamina. In contrast, the apicobasal axes of pm8 and vpi1 are reoriented during morphogenesis. The basal surfaces of pm8 and vpi1 shift to face each other, and presumably form the basal lamina that nearly separates the two cells. This shift in polarity allows pm8 to have obliquely oriented myofilaments; similar myofilaments occur at the terminus of the pharynx in diverse groups of nematodes and are believed to function in moving foodstuffs during feeding (Doncaster, 1962; Mapes, 1965). We speculate that it is advantageous for pm8 and vpi1 to be toroids, rather than simply C-shaped cells, because toroids present a symmetrical pm8/vpi1 interface for cell attachment and basal lamina deposition (see Figure 6A).

Formation of a toroid requires at least one fusion event; thus, pm8 and vpi1 must self-fuse, but not crossfuse. We have shown that pm8 and vpi1 self-fuse by expressing different fusogens, an elegant solution to the problem of creating linked, single-cell tubes. vpi1 expresses a fusogen, EFF-1, that is sufficient to fuse heterologous cells that each express EFF-1 (Podbilewicz et al., 2006). We have shown that in *eff-1* mutants vpi1 is a C-shaped cell with an autocellular junction, indicating that EFF-1 normally promotes the self-fusion of vpi1. pm8 does not express EFF-1, but instead expresses a second fusogen, AFF-1, and requires *aff-1* activity to become a toroid. Thus, AFF-1 and EFF-1 cause self-fusion in pm8 and vpi1, in addition to promoting crossfusion between other types of embryonic cells.

## Epithelial to Mesenchymal Transition

pm8 and vpi1 are wedge-shaped, dorsal epithelial cells prior to becoming C-shaped cells and self-fusing. To form a C-shape around the cyst midline, both pm8 and vpi1 invade between cells in the ventral side of the cyst. Although vpi1 extends only a lamellar process through ventral cells, the nucleus and most of the pm8 cell body enter the ventral side. Notch activity appears to be involved in pm8 delamination from the dorsal basal lamina; pm8 normally detaches from the dorsal perimeter at about the same time as Notch target genes are expressed in pm8, but does not appear to detach in Notch mutant embryos. The delamination and migration of pm8 can be considered an epithelial to mesenchymal transition (EMT). In most animals, EMT is a fundamental and widely used morphogenetic program that functions in gastrulation, and tissue and organ development. EMT also occurs in pathological states during wound healing and in tumor progression (Thiery and Sleeman, 2006). A well-documented role for EMT occurs in the development of the vertebrate heart (Eisenberg and Markwald, 1995). Within the primitive heart tube, epithelial (endocardial) cells that contribute to valve development and heart septation break adherens connections to their neighbors and invade the surrounding extracellular matrix (cardiac jelly). Notch signaling occurs within the endocardium and is critical for EMT (Timmerman et al., 2004). In contrast to

the prevalence of EMT in other systems, the *C. elegans* literature is almost devoid of examples of EMT. For example, most gastrulating cells in *C. elegans* are not epithelial, and lineage mechanisms ensure that most cells are born in their appropriate positions without extensive tissue remodeling (Nance et al., 2005). Because many basic processes in EMT are poorly understood, such as the restructuring of junctional complexes between cells, pm8 morphogenesis should prove a useful model system for genetic analysis.

### Laminin and Intraepithelial Cell Movements

The migration of pm8 and vpi1 between cells in the ventral epithelium of the cyst resembles transepithelial migration in other systems, such as human leukocytes and *Drosophila* germ cells (see Introduction). In all three systems, migration occurs between cells in the target epithelium. These events occur rapidly, requiring about 15 min for pm8 migration and from 5–16 min in some in vitro models of leukocyte invasion (Shaw et al., 2001). In *Drosophila*, the target epithelium appears primed for invasion; apical junctions are remodeled to create intercellular gaps even in the absence of the invading germ cells (Kunwar et al., 2006). In contrast, invading leukocytes can induce junctional remodeling of the target epithelium (Shaw et al., 2001). In our present study, we found (1) that a tract of laminin appears between the ventral cells mc3V and vpi2V prior to pm8 and vpi1 migration, (2) that pm8 and vpi1 migration occurs specifically at the mc3V/vpi2V interface, and is associated with a disappearance of the laminin tract, and (3) that laminin function is essential for pm8 migration (vpi1 was not examined in this experiment). These results suggest that laminin provides a transient path for pm8 migration. We do not yet know whether the formation of the laminin tract is induced by signals from pm8 and/or vpi1, however, the tract forms independent of Notch. Future genetic studies should reveal the laminin receptor(s) involved in pm8 migration. If integrin were the sole receptor for laminin in pm8 migration, we would have expected a lack of migration in integrin mutants, rather than the overmigration, or aberrant migration observed. Interestingly, neurons in $\alpha$6 integrin null mice show an analogous overmigration phenotype (Georges-Labouesse et al., 1998). Although laminin is often implicated in animal cell migration, we know of no similar example of a transient laminin tract guiding migrating cells through a polarized epithelium. The tract in *C. elegans* forms and disappears within about 30 min, so it is possible similar, transient tracts might have been overlooked in epithelia in other systems. Indeed, we observed additional examples of laminin within *C. elegans* tissues that are not known to contain migratory cells (unpublished data). Thus, it will be interesting to determine whether laminin-dependent, short-range cell movements similar to those of pm8 and vpi1 are a common feature of epithelial remodeling.

### Lumen Formation in a Single-Cell Tube

Single-cell tubes are found in diverse animal tissues, including the fine capillaries of the vertebrate vascular system, the termini of the *Drosophila* tracheal system, and the *C. elegans* excretory (renal) system (Lubarsky and Krasnow, 2003). Some of these tubes, such as the fusion cells of the *Drosophila* tracheal system, are toroids like the *C. elegans* pm8 and vpi1 cells (Samakovlis et al., 1996). The lumen in some single-cell tubes is thought to form from the coalescence of cytoplasmic vacuoles (Lubarsky and Krasnow, 2003; Berry et al., 2003; Kamei et al., 2006). In our electron microscopic study, we did not find obvious cytoplasmic vacuoles in pm8 or vpi1 before or immediately after lumen formation (see Figure S3D). pm8 migrates into the ventral side of the epithelial cyst on the left side of the midline, and the pm8 cell body subsequently spreads across the diameter of the cyst. During these events, the three group 3 marginal cells extend fingers posteriorly along the midline. Thus, pm8 must actively or passively wrap around the fingers at the midline. An intriguing possibility is that the fingers play a morphogenetic role in templating the lumenal surface of pm8. However, we have not been able to test this hypothesis by removing all three of the marginal cells simultaneously. If the fingers do not play a direct role in templating the lumen, it is possible they have a mechanical function in holding cyst cells together while pm8 and vpi1 remodel their apical junctions.

### Notch Signaling and Tubulogenesis

The Notch pathway is required for proper pm8 and vpi1 tubulogenesis, and appears to have two distinct roles. First, Notch is required for pm8 to express the fusogen AFF-1. Although the presumptive ligand-expressing cells in the cyst appear to contact both pm8 and vpi1 (see Figure 3C), only pm8 expresses LIN-12/Notch, and only pm8 expresses the Notch targets *ceh-24* and *ref-1*. These results suggest that the Notch pathway is activated only in pm8, and that defects in vpi1 morphogenesis in Notch mutants occur indirectly. Second, we have shown that expression of the EFF-1 fusogen is normally restricted to vpi1, but that pm8 and vpi1 both express EFF-1 in Notch mutants and can crossfuse. Crossfusion would prevent a basal lamina from forming between pm8 and vpi1, and thus account for the inappropriate, broad cellular contacts observed between pharyngeal and valve cells in Notch mutant embryos. Future studies should elucidate the transcriptional network linking Notch targets with fusogen expression and myogenesis. The regulatory regions of both *aff-1* and *eff-1* contain candidate LAG-1/CSL binding sites (unpublished data), however, we do not yet know whether either gene is a direct target of Notch. pm8 does not appear to express FOS-1A, a transcription factor that regulates *aff-1* expression in a larval cell called the anchor cell (Sapir et al., 2007, and unpublished data).

We conclude by noting that cells acquire several distinct and reproducible morphologies during the differentiation of the pharynx/valve from an epithelial cyst. The remarkable number of events underlying the development of just two of these cells, pm8 and vpi1, hint at the complexity of organ differentiation. Because only a few postmitotic cells in the cyst express the receptors LIN-12/Notch or GLP-1/Notch, it appears that Notch does not play a major role in the morphogenesis of most other cyst cells. Thus, it is likely that there are several different pathways that specify cell shapes throughout the cyst, and it should be interesting in future studies to identify these pathways and determine how they are coordinated.

## EXPERIMENTAL PROCEDURES

### Nematodes

Standard techniques were used to maintain and manipulate nematodes (Brenner, 1974). The following extrachromosomal or integrated arrays were created

for this study; details available upon request: *zuEx146*: [*ceh-24* $^{115bp}$::GFP (pKG63); *rol-6*], *zuEx165*: [*ceh-24* $^{115bp\ (-CSL)}$::GFP (pKG70); *rol-6*], *zuEx221*: [*ref-1*$^{153bp}$::GFP-PM (pKG79); *rol-6*], *zuIs190:* [*myo-2*::GFP (pSEM474); *rol-6*]; the plasmid pSEM474 was kindly provided by Jeb Gaudet and Susan Mango. The following transgenes have been described: *zuEx132*: [*ref-1*$^{(600bp)}$::GFP] (Neves et al., 2007); *zuIs104*: [*ref-1*$^{(1.8kb)}$::REF-1::GFP] (Neves and Priess, 2005); *urEx131*: [*lam-1*::LAM-1::GFP] (Kao et al., 2006); *hyEx167*: [*aff-1*::GFP] (Sapir et al., 2007); *zzIs22*: [*eff-1*::EFF-1::GFP] (del Campo et al., 2005); and *syIs123:* [*fos-1a*::YFP::FOS-1A] (Sherwood et al., 2005). Mutant alleles used in this study are described in WormBase (http://www.wormbase.org/): LG1, *lam-3(n2561)*; LG II, *aff-1(tm2214)*, *eff-1(hy21), eff-1(ok1021)*; LG III, *glp-1(q46), ina-1(gm86), lin-12(n941)*; LG IV, *epi-1(rh199)*, *lag-1(q385)*; LG V, *apx-1(zu347ts), lag-2(q387), lag-2(q411)*, *lag-2(q420ts)*. A strain was constructed with the *ref-1*::GFP-PM transgene that was heterozygous for the *lam-3(n2561)* and *epi-1(rh199)* mutations. Approximately 1/16 of the progeny of these animals had a novel and consistent defect in pm8 migration that was not observed in either of the homozygous single mutants; we infer that these embryos are homozygous for both mutations.

### Transgenes

Standard techniques were used to manipulate DNA. All transgene constructs were made using PCR fusion techniques (Hobert, 2002). GFP reporter constructs for *ceh-24* and *ref-1* were derived from pAP10 (A. Paulson and S.E. Mango, unpublished data). The *ceh-24* promoter was amplified using PstI linkers and the following forward (F) and reverse (R) genomic sequences: *ceh-24* (F = gagctctttgcatctttttcac, R = gagaagtgttatcagtgttatcc; pKG63). *ref-1*::GFP-PM was constructed by cloning amplified genomic *ref-1* DNA (F = ctcaccaggggttatcaaaccaatatg, R = atcccaatggttcccatcactatc) into the Hind III/Bam H1 sites of pJN152 GFP-PM (J. Nance, unpublished data). Promoter / enhancer mutagenesis was performed using the QuikChange site-directed mutagenesis kit (Stratagene, La Jolla, CA, USA). Predicted start codons were obtained from the WormBase web site (http://www.wormbase.org). Constructs were injected at 40 ng/μl together with *rol-6* DNA, at 100 ng/μl, to generate extrachromosomal arrays (Mello and Fire, 1995). At least two independent lines were analyzed for each transgene, and at least 20 embryos were examined per line. The *myo-2*::GFP array was integrated by $\gamma$ irradiation (Mello and Fire, 1995).

Electrophoretic mobility shift assays (EMSA) shown in Figure S1 were performed essentially as described (Stroeher et al., 1994), but see the Supplemental Data for details.

### Immunofluorescence

The following antibodies/antisera were used: anti-LAM-3, anti-EPI-1 (Huang et al., 2003), mAbGJ1, mAbGJ2 (see Supplemental Experimental Procedures), anti-LIN-12 (gift from Stuart Kim), MH27 (Francis and Waterston, 1991), anti-GFP (Abcam ab6556). Worm and embryo fixation procedures were performed essentially as described (Lin et al., 1998; Leung et al., 1999). Unless stated otherwise, between 5 and 25 embryos were analyzed for all immunofluorescence experiments.

### Microscopy

Electron microscopy was performed as described (Costa et al., 1997). Sets of 5–10 thin sections spaced by 0.5–1 micron intervals were taken from plastic-embedded clusters of 25–50 embryos. Embryos with the plane of section though the axis of the pharyngeal lumen were selected for detailed analysis.

Images shown in Figure S4 and Figure 4F were from a set of serial sections through the terminal bulb of the pharynx and valve (J.R.P. and J.N. Thomson, unpublished data). Fluorescence images in Figure 5G and Movies S1, S2, and S4 were collected with a spinning disk confocal system (Yokogawa CSU-10) on a Nikon TE-2000 inverted microscope equipped with a Hamamatsu C-9100 camera, running Volocity 4.1 (Improvision, Lexington, MA).

## SUPPLEMENTAL DATA

Supplemental Data include four figures, four movies, and Supplemental Experimental Procedures and can be found with this article online at http://developmentalcell.com/cgi/content/full/14/4/559/DC1/.

## ACKNOWLEDGMENTS

We thank Jeremy Nance for advice about laminin localization, an anonymous reviewer for comments about autocellular junctions, A. Chisholm and W. Wadsworth for strains and antisera, and members of the Priess lab for discussion and technical assistance. We thank Jeff Molk for assistance with confocal microscopy. Some of the nematode strains used in this study were provided by the *Caenorhabditis* Genetics Center, which is funded by the NIH National Center for Research Resources. J.P.R. and J.R.T. were supported by National Institutes of Health Developmental Biology Training Grant 5T32 HDO7183. J.R.P. is an investigator with HHMI.

Received: July 23, 2007
Revised: October 22, 2007
Accepted: January 31, 2008
Published: April 14, 2008

## REFERENCES

Albertson, D.G., and Thomson, J.N. (1976). The pharynx of *Caenorhabditis elegans*. Philos. Trans. R. Soc. Lond. B Biol. Sci. *275*, 299–325.

Alper, S., and Kenyon, C. (2001). REF-1, a protein with two bHLH domains, alters the pattern of cell fusion in *C. elegans* by regulating Hox protein activity. Development *128*, 1793–1804.

Berry, K.L., Bulow, H.E., Hall, D.H., and Hobert, O. (2003). A *C. elegans* CLIC-like protein required for intracellular tube formation and maintenance. Science *302*, 2134–2137.

Bray, S.J. (2006). Notch signalling: a simple pathway becomes complex. Nat. Rev. Mol. Cell Biol. *7*, 678–689.

Brenner, S. (1974). The genetics of *Caenorhabditis elegans*. Genetics *77*, 71–94.

Casanova, J. (2007). The emergence of shape: notions from the study of the *Drosophila* tracheal system. EMBO Rep. *8*, 335–339.

Chen, J.N., and Fishman, M.C. (1996). Zebrafish *tinman* homolog demarcates the heart field and initiates myocardial differentiation. Development *122*, 3809–3816.

Costa, M., Draper, B.W., and Priess, J.R. (1997). The role of actin filaments in patterning the *Caenorhabditis elegans* cuticle. Dev. Biol. *184*, 373–384.

del Campo, J.J., Opoku-Serebuoh, E., Isaacson, A.B., Scranton, V.L., Tucker, M., Han, M., and Mohler, W.A. (2005). Fusogenic activity of EFF-1 is regulated via dynamic localization in fusing somatic cells of *C. elegans*. Curr. Biol. *15*, 413–423.

Doncaster, C.C. (1962). Nematode feeding mechanisms. I. Observations on Rhabditis and Pelodera. Nematologica *8*, 313–320.

Eisenberg, L.M., and Markwald, R.R. (1995). Molecular regulation of atrioventricular valvuloseptal morphogenesis. Circ. Res. *77*, 1–6.

Francis, R., and Waterston, R.H. (1991). Muscle cell attachment in *Caenorhabditis elegans*. J. Cell Biol. *114*, 465–479.

Georges-Labouesse, E., Mark, M., Messaddeq, N., and Gansmuller, A. (1998). Essential role of $\alpha$6 integrins in cortical and retinal lamination. Curr. Biol. *8*, 983–986.

Gong, Y., Mo, C., and Fraser, S.E. (2004). Planar cell polarity signaling controls cell division orientation during zebrafish gastrulation. Nature *430*, 689–693.

Greenwald, I. (August 4, 2005). LIN-12/Notch signaling in *C. elegans, WormBook*, ed. The *C. elegans* Research Community, WormBook. doi/10.1895/wormbook.1.10.1. http://www.wormbook.org.

Harfe, B.D., and Fire, A. (1998). Muscle and nerve-specific regulation of a novel NK-2 class homeodomain factor in *Caenorhabditis elegans*. Development *125*, 421–429.

Haun, C., Alexander, J., Stainier, D.Y., and Okkema, P.G. (1998). Rescue of *Caenorhabditis elegans* pharyngeal development by a vertebrate heart specification gene. Proc. Natl. Acad. Sci. USA *95*, 5072–5075.

Hobert, O. (2002). PCR Fusion-based approach to create reporter gene constructs for expression analysis in transgenic *C. elegans*. Biotechniques *32*, 728–730.

Horner, M.A., Quintin, S., Domeier, M.E., Kimble, J., Labouesse, M., and Mango, S.E. (1998). *pha-4*, an HNF-3 homologue, specifies pharyngeal organ identity in *Caenorhabditis elegans*. Genes Dev. *12*, 1947–1952.

Huang, C.C., Hall, D.H., Hedgecock, E.M., Kao, G., Karantza, V., Vogel, B.E., Hutter, H., Chisholm, A.D., Yurchenco, P.D., and Wadsworth, W.G. (2003). Laminin $\alpha$ subunits and their role in *C. elegans* development. Development *130*, 3343–3358.

Kalb, J.M., Lau, K.K., Goszczynski, B., Fukushige, T., Moons, D., Okkema, P.G., and McGhee, J.D. (1998). *pha-4* is *Ce-fkh-1*, a *fork head/HNF-3*$\alpha$, $\beta$, $\gamma$ homolog that functions in organogenesis of the *C. elegans* pharynx. Development *125*, 2171–2180.

Kamei, M., Saunders, W.B., Bayless, K.J., Dye, L., Davis, G.E., and Weinstein, B.M. (2006). Endothelial tubes assemble from intracellular vacuoles *in vivo*. Nature *442*, 453–456.

Kao, G., Huang, C.C., Hedgecock, E.M., Hall, D.H., and Wadsworth, W.G. (2006). The role of the laminin $\beta$ subunit in laminin heterotrimer assembly and basement membrane function and development in *C. elegans*. Dev. Biol. *290*, 211–219.

Kramer, J.M. (September 1, 2005). Basement membranes, *Wormbook*, ed. The *C. elegans* Research Community, WormBook. doi/10.1895/wormbook.1.16.1. http://www.wormbook.org.

Kunwar, P.S., Siekhaus, D.E., and Lehman, R. (2006). In vivo migration: a germ cell perspective. Annu. Rev. Cell Dev. Biol. *22*, 237–265.

Leung, B., Hermann, G.J., and Priess, J.R. (1999). Organogenesis of the *Caenorhabditis elegans* intestine. Dev. Biol. *216*, 114–134.

Lin, R., Hill, R.J., and Priess, J.R. (1998). POP-1 and anterior-posterior fate decisions in *C. elegans* embryos. Cell *92*, 229–239.

Lubarsky, B., and Krasnow, M.A. (2003). Tube morphogenesis: making and shaping biological tubes. Cell *112*, 19–28.

Mango, S.E. (January 22, 2007). The *C. elegans* pharynx: a model for organogenesis. *Wormbook*, ed. The *C. elegans* Research Community, WormBook. doi/10.1895/wormbook.1.129.1. http://www.wormbook.org.

Mango, S.E., Lambie, E.J., and Kimble, J. (1994). The *pha-4* gene is required to generate the pharyngeal primordium of *Caenorhabditis elegans*. Development *120*, 3019–3031.

Mapes, C.J. (1965). Structure and function in the nematode pharynx. I. The structure of the pharynges of *Ascaris lumbricoides, Oxyuris equi, Apectana brevicaudata* and *Panagrellus silusiae*. Parasitology *55*, 269–284.

Mello, C., and Fire, A. (1995). DNA transformation. In *Caenorhabditis elegans*: Modern Biological Analysis of an Organism, H.F. Epstein and D.C. Shakes, eds. (San Diego, CA: Academic Press), pp. 452–482.

Mohler, W.A., Shemer, G., del Campo, J.J., Valansi, C., Opoku-Serebuoh, E., Scranton, V., Assaf, N., White, J.G., and Podbilewicz, B. (2002). The type I membrane protein EFF-1 is essential for developmental cell fusion. Dev. Cell *2*, 355–362.

Nance, J., Lee, J.-Y., and Goldstein, B. (September 26, 2005). Gastrulation in *C. elegans. WormBook*, ed. The *C. elegans* Research Community, WormBook. doi/10.1895/wormbook.1.23.1. http://www.wormbook.org.

Neves, A., and Priess, J.R. (2005). The REF-1 family of bHLH transcription factors pattern *C. elegans* embryos through Notch-dependent and Notch-independent pathways. Dev. Cell *8*, 867–879.

Neves, A., English, K., and Priess, J.R. (2007). Notch-GATA synergy promotes endoderm-specific expression of *ref-1* in *C. elegans*. Development *134*, 4459–4468.

Oliphant, L.W., and Cloney, R.A. (1972). The ascidian myocardium: Sarcoplasmic reticulum and excitation-contraction coupling. Z. Zellforsch. *129*, 395–412.

Okkema, P.G., and Fire, A. (1994). The *Caenorhabditis elegans NK-2* class homeoprotein CEH-22 is involved in combinatorial activation of gene expression in pharyngeal muscle. Development *120*, 2175–2186.

Okkema, P.G., Ha, E., Haun, C., Chen, W., and Fire, A. (1997). The *Caenorhabditis elegans NK-2* homeobox gene *ceh-22* activates pharyngeal muscle gene expression in combination with *pha-1* and is required for normal pharyngeal development. Development *124*, 3965–3973.

Petri, B., and Bixel, M.G. (2006). Molecular events during leukocyte diapendesis. FEBS J. *273*, 4399–4407.

Podbilewicz, B., Leikina, E., Sapir, A., Valansi, C., Suissa, M., Shemer, G., and Chernomordik, L.V. (2006). The *C. elegans* developmental fusogen EFF-1 mediates homotypic fusion in heterologous cells and in vivo. Dev. Cell *11*, 471–481.

Portereiko, M.F., and Mango, S.E. (2001). Early morphogenesis of the *Caenorhabditis elegans* pharynx. Dev. Biol. *233*, 482–494.

Priess, J. (2005). Notch signaling in the *C. elegans* embryo. *WormBook*, ed. The *C. elegans* Research Community, WormBook. doi/10.1895/wormbook.1.4.1. http://www.wormbook.org.

Priess, J.R., Schnabel, H., and Schnabel, R. (1987). The *glp-1* locus and cellular interactions in early *C. elegans* embryos. Cell *51*, 601–611.

Samakovlis, C., Manning, G., Steneberg, P., Hacohen, N., Cantera, R., and Krasnow, M.A. (1996). Genetic control of epithelial tube fusion during *Drosophila* tracheal development. Development *122*, 3531–3536.

Sapir, A., Choi, J., Leikina, E., Avinoam, O., Valansi, C., Chernomordik, L.V., Newman, A.P., and Podbilewicz, B. (2007). AFF-1, a FOS-1-regulated fusogen, mediates fusion of the anchor cell in *C. elegans*. Dev. Cell *12*, 683–698.

Schreiber, A.M., Cai, L., and Brown, D.D. (2005). Remodeling of the intestine during metamorphosis of *Xenopus laevis*. Proc. Natl. Acad. Sci. USA *102*, 3720–3725.

Shaw, S.K., Bamba, P.S., Perkins, B.N., and Luscinskas, F.W. (2001). Real-time imaging of vascular endothelial-cadherin during leukocyte transmigration across endothelium. J. Immunol. *167*, 2323–2330.

Sherwood, D.R., Butler, J.A., Kramer, J.M., and Sternberg, P.W. (2005). FOS-1 promotes basement-membrane removal during anchor-cell invasion in *C. elegans*. Cell *121*, 951–962.

Stroeher, V.L., Kennedy, B.P., Millen, K.J., Schroeder, D.F., Hawkins, M.G., Goszczynski, B., and McGhee, J.D. (1994). DNA-protein interactions in the *Caenorhabditis elegans* embryo: Oocyte and embryonic factors that bind to the promoter of the gut-specific *ges-1* gene. Dev. Biol. *163*, 367–380.

Thiery, J.P., and Sleeman, J.P. (2006). Complex networks orchestrate epithelial-mesenchymal transitions. Nat. Rev. Mol. Cell Biol. *7*, 131–142.

Timmerman, L.A., Grego-Bessa, J., Raya, A., Bertran, E., Perez-Pomares, J.M., Diez, J., Aranda, S., Palomo, S., McCormick, F., Izpisua-Belmonte, J.C., and de la Pompa, J.L. (2004). Notch promotes epithelial-mesenchymal transition during cardiac development and oncogenic transformation. Genes Dev. *18*, 99–115.